WILEY-VCH

Edited by
Sushil K. Misra

Multifrequency Electron Paramagnetic Resonance

Data and Techniques

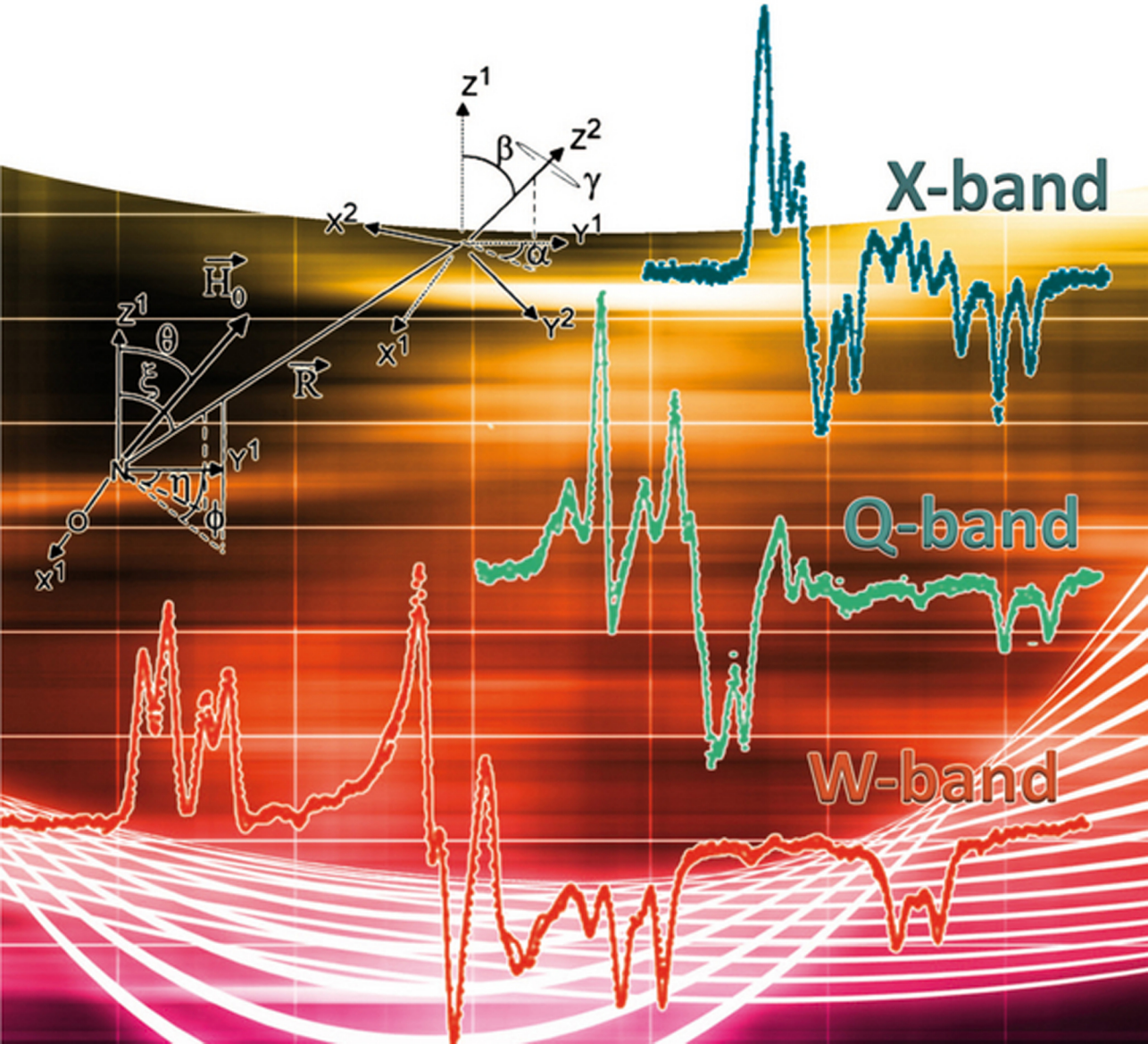

Edited by
Sushil K. Misra

Multifrequency Electron Paramagnetic Resonance

Related Titles

Misra, S.K. (ed.)

Multifrequency Electron Paramagnetic Resonance

Theory and Applications

2011
Print ISBN: 978-3-527-40779-8
ISBN: 978-3-527-63353-1
Adobe PDF ISBN: 978-3-527-63354-8
ePub ISBN: 978-3-527-63355-5
eMobi ISBN: 978-3-527-64049-2

Edited by Sushil K. Misra

Multifrequency Electron Paramagnetic Resonance

Data and Techniques

WILEY-VCH
Verlag GmbH & Co. KGaA

The Editor

Sushil K. Misra
Concordia University
Department of Physics
1455 de Maisonneuve Boulevard
West
Montreal
Quebec H3G 1M8
Canada

Library of Congress Card No.: applied for

British Library Cataloguing-in-Publication Data
A catalogue record for this book is available from the British Library.

Bibliographic information published by the Deutsche Nationalbibliothek
The Deutsche Nationalbibliothek lists this publication in the Deutsche Nationalbibliografie; detailed bibliographic data are available on the Internet at <http://dnb.d-nb.de>.

Print ISBN: 978-3-527-41222-8
ePDF ISBN: 978-3-527-67244-8
ePub ISBN: 978-3-527-67245-5
Mobi ISBN: 978-3-527-67246-2
oBook ISBN: 978-3-527-67243-1

Cover Design Adam-Design, Weinheim, Germany
Typesetting Laserwords Private Limited, Chennai, India
Printing and Binding Markono Print Media Pte Ltd., Singapore

Printed on acid-free paper

Contents

Preface

Research into electron paramagnetic resonance (EPR), also known as *electron spin resonance* (*ESR*) and *electron magnetic resonance* (*EMR*), has been constantly expanding since the first article on this topic by Zavoisky in 1945. The field of EPR imaging, previously considered unachievable, is now well developed, complementing MRI (magnetic resonance imaging), a development of NMR (nuclear magnetic resonance), based on the resonance of protons possessing a nuclear magnetic moment. Moreover, EPR finds extensive applications in biology, medicine, chemistry, physics, and geology. It is, therefore, important to provide the scientific community with information on the latest developments in the field of EPR.

This volume is in continuation of the efforts put forward by my colleagues C. P. Poole, Jr. and H. A. Farach, who edited ESR Handbooks (ESRHB), Volume 1 (AIP Press, New York, 1994) and Volume 2 (Springer, AIP Press, New York, 1999), and by myself, editing the book ''Multifrequency Electron Paramagnetic Resonance: Theory and Applications'' (MFEPRTA; Wily-VCH, Weinheim, Germany, 2011). ESRHB Volume 1 dealt with the general aspects of the literature, with chapters on computer techniques, relaxation, and electron-nuclear double resonance (ENDOR), whereas Volume 2 contained chapters on sensitivity, resonators, lineshapes, electron-spin-echo envelope modulation (ESEEM), transition metal (TM) ion series, spin-Hamiltonian (SH) types and symmetries, evaluation of SH parameters from EPR data, EPR imaging, high-field EPR, and a thorough tabulation of TM ion data on SH parameters till 1993. Since the publication of these handbooks the technique of multifrequency EPR has been used extensively in EPR research. As for MFEPRTA book, it covered extensively the latest developments in theory and applications of multifrequency EPR. The present volume is aimed to provide chapters on the latest state-of-the-art information on EPR. It covers the technique of rapid-scan EPR and a thorough coverage of the literature on compilation of multifrequency EPR spectra and evaluation of SH parameters, as well as an exhaustive tabulation of TM ion SH parameters covering the period of 20 years (1993–2012, inclusive). In addition, a small chapter is devoted to a tabulation of hyperfine splittings and g-factors of some typical aminoxyl (nitroxide) ions published over the years. It is hoped that this volume will serve a useful and timely purpose to EPR researchers at large.

I am grateful to Professor C. P. Poole, Jr., University of South Carolina, for his constant mentoring throughout my efforts to put together this volume. Thanks are also due to Danielle Dennie and Katharine Hall, reference librarians at Concordia University, for their searches through the various databases to find the relevant articles.

Finally, I dedicate this book to my parents Mr. Rajendra Misra and (late) Mrs. Prakash Wati Misra, my daughters Manjula and Shivali, and my son Paraish.

List of Contributors

Lawrence J. Berliner
Department of Chemistry and Biochemistry
2190 E Iliff Ave
University of Denver
Denver
CO 80208
USA

Stefan Diehl
Justus Liebig University Griessen
2nd Physics Institute
Heinrich-Buff-Ring 16
35392 Griessen, Germany

Gareth R. Eaton
Department of Chemistry and Biochemistry
University of Denver
Denver
CO 80208
USA

Sandra S. Eaton
Department of Chemistry and Biochemistry
University of Denver
Denver
CO 80208
USA

Sushil K. Misra
Concordia University
Department of Physics
1455 de Maisonneuve Boulevard West
Montreal
Quebec H3G 1M8
Canada

Deborah G. Mitchell
Department of Chemistry and Biochemistry
University of Denver
Denver
CO 80208
USA

Sean Moncrieff
Concordia University
Physics Department
1455 de Maisonneuve Boulebard West
Montreal
Quebec H3G 1M8
Canada

Richard W. Quine
Daniel Felix Ritchie School of Engineering and Computer Science
University of Denver
Denver
CO 80208
USA

George A. Rinard
Daniel Felix Ritchie School of Engineering and Computer Science
University of Denver
Denver
CO 80208
USA

Stefan Stoll
University of Washington
Department of Chemistry
Seattle
WA 98195
USA

Mark Tseitlin
Department of Chemistry and Biochemistry
University of Denver
Denver
CO 80208
USA

1
Introduction

Sushil K. Misra

This volume consists of five chapters including the introduction, covering the various aspects of the technique of EPR (electron paramagnetic resonance, also known as ESR – electron spin resonance and EMR – electron magnetic resonance), in a timely manner. The most notable feature in this context is the multifrequency aspect of the contents, which is now the practice in EPR research. The various chapters are briefly described here.

1) **Recording of EPR spectra using the recently developed techniques in rapid scan**. In this chapter (Chapter 2), the background, theory, instrumentation, and methodology of rapid-scan EPR, including the hardware and software required to implement rapid scans and analysis of the data, are described. Among other advantages, the ability of rapid scans to acquire data quickly permits higher temporal resolution for kinetics than can be achieved with CW (continuous wave) spectroscopy. In rapid-scan EPR, the magnetic field is scanned through resonance in a time that is short relative to electron spin-relaxation times. Direct detection of the EPR response yields the absorption and dispersion signals, instead of the derivatives that are recorded in the usual CW experiment. The rapid-scan signal provides the full amplitude of EPR absorption, and not just a small approximately linear segment as is recorded in field-modulated EPR. In a rapid scan, if the time on resonance is short relative to relaxation times, there is a scan-rate dependence response that can be deconvolved to yield the undistorted absorption signal. If the time on resonance is long enough that the signal is independent of scan rate, the deconvolution procedure does not change the spectrum; therefore, the data analysis method is general for any rate of passage through resonance. The signal-to-noise ratios obtained by rapid scan are higher by factors of as much as 20 to >250 than those obtained by CW EPR for samples ranging from spin-trapped superoxide and nitroxide radicals in fluid solution to paramagnetic centers in materials.
2) **Simulation of EPR spectra and evaluation of spin-Hamiltonian parameters (SHP)** as developed over the years. After summarizing the key aspects of available simulation software packages, the basic aspects of EPR simulations are discussed in Chapter 3. Thereafter, methods for simulation of static and

Multifrequency Electron Paramagnetic Resonance: Data and Techniques, First Edition.
Edited by Sushil K. Misra.

dynamic CW EPR, pulse EPR, ENDOR (electron nuclear double resonance), and DEER (double electron electron resonance) spectra are described. Subsequently, a section is dedicated to least-squares fitting. After a short section covering topics such as spin quantization and data formats, some of the challenges that still lie ahead are summarized in the conclusion. This chapter provides an expert overview of computational modeling and least-squares fitting of EPR spectra. A well-written summary of the theory and methods involved in EPR spectral simulation, covering a wide range of regimes (solids, liquids, slow motion, chemical exchange), experiments (cw and pulse EPR, ENDOR), and methods (Liouville space, Hilbert space, matrix diagonalization, perturbation theory) is provided. The discussion of least-squares fitting includes many aspects that are often only discussed in isolation. Apart from the author's very general and widely used software package EasySpin, many other existing programs are mentioned. The chapter concludes with an extensive list of over 500 references that encompasses not only the seminal high-impact papers from the last half century but also many less known contributions.

3) Chapter 4 is devoted to an exhaustive *tabulation of Spin-Hamiltonian parameters (SHPs) of transition metal ions*, as published in the last 20 years (1993–2012, inclusive). It supplements a similar data listing published in the *ESR Handbook*, Volume 2, edited by C. P. Poole, Jr. and H. A. Farach (Springer, AIP Press, New York, 1999), which covers the period from 1960s to 1992. Since then, in contrast, the technique of multifrequency EPR has been used extensively in EPR research. This information is useful for various purposes, which includes verification of new EPR results, planning of experiments, and finding what parameters have been reported in the literature, without having to do an extensive database search that may quite frequently involve journals that are not readily available.
4) Finally, Chapter 5 contains a tabulation of *hyperfine splitting and g-factors of some typical aminoxyl (nitroxide) radicals*. Since the first *Spin Labeling: Theory and Applications* volume in 1976, edited by L. Berliner, no compilation has been published on this topic. With the use of organic radicals such as spin labels, calibration agents, and so on, a complete reference listing of their physical parameters is useful. In particular, the aminoxyl (nitroxide) radicals are stable organic compounds that have found a plethora of uses in chemistry, biology, and physics. The compiled data, while not thorough, cover a range of these radical types at several frequencies, solvent environments, and hosts. In some selected cases, where the data were readily available, parameters in several host environments, solvents, and other states have been included, since polarity affects both the hyperfine and g-values.

2
Rapid-Scan Electron Paramagnetic Resonance

Sandra S. Eaton, Richard W. Quine, Mark Tseitlin, Deborah G. Mitchell, George A. Rinard, and Gareth R. Eaton

2.1
Introduction

The focus of this chapter is on the emerging and very powerful implementation of electron paramagnetic resonance (EPR) that is designated as rapid scan. Historically, most EPR instrumentation and methodology have been in one of two regimes: continuous wave (CW) [1, 2], or pulsed (saturation recovery, spin echo, and Fourier Transform) [3–6]. In a CW experiment the microwave power is constant, the magnetic field is scanned to achieve resonance, and the EPR signal is recorded by phase-sensitive detection at the frequency that is used for magnetic field modulation. Microwave powers and scan rates are selected such that spectra are independent of relaxation times. In pulse experiments, the microwave power is on only during excitation, signals are detected after the pulse(s), and differences in relaxation times are exploited to optimize information content. The rapid-scan regime is an intermediate case. As in CW experiments the microwave power is constant, but the magnetic field (or microwave frequency) is scanned through resonance in a time that is short relative to relaxation times, and phase-sensitive detection at a magnetic field modulation frequency is not used. Instead, the absorption and dispersion signals are recorded by direct detection with a double balanced mixer. Rapid scans and data analysis as discussed in the following paragraphs permit spectral acquisition with lineshapes that are not modulation broadened and have substantially improved signal-to-noise ratio (S/N) relative to CW spectroscopy. These experiments can be performed without the use of the high powers that are required for pulse experiments. In pulse experiments, data acquisition requires samples for which the decay time for a free induction decay (FID), T_2*, is long relative to the instrument dead time. This is not a limitation for rapid scans. The combination of rapid scan with improvements in digital electronics provides opportunities to revolutionize the way that much EPR will be done in the future.

Historical development, analysis of data to recover the equivalent slow-scan spectrum, and hardware modifications of conventional spectrometers to implement

Multifrequency Electron Paramagnetic Resonance: Data and Techniques, First Edition.
Edited by Sushil K. Misra.

rapid scans are discussed in this chapter. The technology and methodology to acquire, deconvolve, and interpret the transient responses are emphasized. In terms of instrumentation, the difference between CW and rapid scan is in the scan coils and drivers, optimized resonators, and detector bandwidth. The Hyde laboratory has developed segmental acquisition of spectra, scanning a few gauss at a time [7], while the Denver laboratory engineered faster and larger magnetic field sweeps to encompass spectra of most organic radicals [8, 9] to improve *S/N* [10, 11], to enhance EPR imaging [12], and to measure relaxation times [13, 14]. Section 2.12 of this chapter provides examples of the dramatic improvements in *S/N* that have been obtained by rapid scans of samples ranging from spin-trapped radicals to paramagnetic centers in materials. Most of the results surveyed are from the Denver laboratory.

2.1.1 Historical Background and Literature Survey

Rapid-scan EPR builds on prior work in NMR (nuclear magnetic resonance). Bloembergen *et al*. [15] observed a transient effect (''wiggles'') after the magnetic field passed through resonance [16]. In 1974, it was shown that these transient effects could be deconvolved to obtain useful NMR spectra (''correlation NMR spectroscopy'' or ''rapid-scan Fourier transform NMR spectroscopy'' (FT-NMR)) [16–19]. Rapid-scan NMR achieved almost as high an *S/N* as pulsed FT-NMR, with the additional advantage that rapid-scan NMR could measure a portion of a spectrum, and hence avoid a strong solvent peak. Rapid-scan NMR was soon eclipsed by FT-NMR owing to the wide range of pulse sequences that became available. However, its use continued in a routine commercial NMR spectrometer.

Transient effects were also observed in the early days of EPR. The first observation of ''wiggles'' in EPR was by Beeler *et al*. [20, 21], using an approximately 25 mG wide line of sodium in liquid ammonia, and scan rates of 1.5×10^4 G s^{-1}. The EPR frequency was 23 MHz (8.2 G resonant field), the amplitude of the sinusoidal field scan was 1.1 G, and the scan frequency was 2 kHz. Effects of rapidly changing fields on signals from sugar char were reported by Gabillard [22]. Gabillard and Ponchel [23] showed that shapes of EPR spectra of DPPH (2,2-diphenyl-1-picrylhydrazyl) changed when the modulation period was comparable to T_2.

There is vast early literature on the effects of adiabatic passage on electron spins, of which a small portion is cited here to provide some background. Adiabatic rapid passage effects were observed in irradiated LiF by Portis [24] and by Hyde [25]. Feher and coworkers used rapid passage effects in electron-nuclear double resonance (ENDOR) experiments [26–28]. Multiple passage effects were described by Weger [29]. Although published 50 years ago, Weger's article remains the only extensive review of passage effects in magnetic resonance. Many cases were illustrated providing sketches of the expected effects on absorption and dispersion EPR spectra. It remains a guide to the range of phenomena that are potentially

observable. In Weger's terminology [29], ''rapid'' refers to the regime in which

$$\frac{B_1}{\left[\left(\frac{dB}{dt}\right)(T_1T_2)^{\frac{1}{2}}\right]} < 1 \tag{2.1}$$

where B is the external magnetic field, t is time, T_1 and T_2 are the electron spin relaxation times, and B_1 is the radio frequency (RF)/microwave magnetic field. Weger [29] defined adiabatic as the regime in which the signal is partially saturated and the scans are characterized by $(\omega_m H_m/\gamma {B_1}^2) << 1$ or $(dB_o/dt)/(\gamma {B_1}^2) << 1$. Thus, in his terminology, most of the scans discussed in this chapter are non-adiabatic. Slow scan is described by

$$\frac{dB}{dt} \ll \gamma(\delta B)^2 \tag{2.2}$$

where δB is the relaxation-determined linewidth expressed in magnetic field units. $\gamma = -1.7609 \times 10^{11}$ rad s^{-1} T^{-1} $= -1.7609 \times 10^{7}$ rad s^{-1} G^{-1} is the free electron gyromagnetic ratio.

Czoch *et al.* [30] observed an EPR transient response for the TCNQ radical (N-methylpyridinium tetracyanoquinodimethane) with a sinusoidal magnetic field scan rate of 2×10^5 G s^{-1}. A low-Q helix was used as the resonator. Saturation transfer EPR exploits passage effects to estimate rotational correlation times of nitroxide radicals [31]. Other applications of rapid passage include ^{57}Fe ENDOR obtained with dispersion derivative EPR under adiabatic rapid passage conditions [32]. Seamonds *et al.* [33] and Mailer and Taylor [34] used adiabatic rapid passage to enhance the intensity of EPR spectra of ferric hemoglobin and ferrocytochrome c, respectively. Signal enhancements in irradiated tooth samples were achieved by second harmonic out-of-phase signal detection at 77 K, using 100 kHz magnetic field modulation [35]. The out-of-phase response under adiabatic rapid passage conditions has been used to enhance intensities of the nitrogen signal in natural diamond [36]. The phase lag of the signal was used to estimate T_1 as 1.7 ± 0.7 ms. Periodic adiabatic passage with monitoring of the dispersion mode 90° out of phase with the modulation was used to measure T_1 of hydrogenated amorphous silicon and silicon carbide [37]. Rapid passage spectra also have been observed in rotational spectroscopy [38] and in infrared spectroscopy [39].

Hyde *et al.* [40] achieved rapid frequency scans, up to 1.8×10^5 GHz/s, in a 94 GHz EPR spectrometer. Rapid triangular and trapezoidal frequency sweeps through nitroxide lines resulted in transient responses (''wiggles''). The National Cancer Institute group of Murali Krishna and coworkers [41, 42] has incorporated rapid-scan and rotating magnetic field gradients into a fast CW EPR imaging method, and found a strong advantage of rapid scan for imaging nitroxide radicals. Direct-detected X-band (9.5 GHz) and L-band (1–2 GHz) absorption EPR spectra have been acquired using scans that are slow relative to relaxation times, that is, non-adiabatic rapid sweeps (NARS), as a replacement for the field-modulated, phase-sensitive-detected derivative CW EPR spectra [7, 43]. With scan rates that satisfy the non-adiabatic condition, pure absorption EPR spectra of nitroxide radicals were collected in magnetic field segments. By avoiding the line broadening

that is inherent in any field-modulated CW spectrum, the L-band nitroxide center line was narrow enough to be sensitive to spin–spin interactions at distances of 18–30 Å [43].

The publications from the Eaton laboratory at the University of Denver (Denver laboratory) have emphasized the cases in which the magnetic field or frequency scan rate is rapid relative to relaxation rates as defined by Weger [29]. There is little or no saturation in most of these spectra, so the conditions are also non-adiabatic. If the time required to scan through the line is short relative to T_2, there are transient effects on the trailing edge of the rapid-scan signal, which damp out with time constant T_2*. In the early literature those oscillations were called *wiggles*. If $T_2^* \ll T_2$, spectra may be in the rapid-scan regime even though oscillations are not observed. Rapid-scan EPR spectra from the Denver laboratory illustrate the impact of relaxation times and microwave power on signal amplitude and shape [10, 14, 44, 45], the impact of resonator parameters [46], the ability to deconvolve signals [47–49], and to reconstruct images from rapid-scan spectra [12]. Since the damping of wiggles depends on T_2 (as well as inhomogeneous broadening), T_2 can be determined from the rapid-scan response [14]. Rapid linear (triangular) [8] and sinusoidal [9] scan drivers have been described.

There also are cases in the literature where the term *rapid* has been used to describe magnetic field or frequency scans that are rapid relative to normal rates of scanning an iron-core magnet [50, 51], but are not rapid relative to relaxation rates. Since the scan rate that is rapid for one sample may be slow for another, similar technology applies in both regimes. The hardware and advances described in this chapter apply in that regime as well. If a spectrum includes lines with different relaxation times such that scan times are short relative to relaxation times for some lines, but not for others, the deconvolution methods described in Section 2.2 can still be applied. This chapter focuses on the observation of transient effects in the EPR spectra of organic radicals in solution and defect centers in solids at room temperature. This is a new regime for EPR, and new aspects of methodology and applications are being developed.

2.1.2
Comparison of CW, Rapid-Scan, and Pulsed EPR: Advantages of Rapid Scan

Traditional CW EPR records the first-derivative of the absorption signal as a function of the slowly scanned Zeeman field, which often takes several minutes. Superimposed on the slowly scanned magnetic field is a sufficiently small, rapidly modulated, magnetic field that encodes the EPR response such that it can be distinguished from noise using phase-sensitive detection at the modulation frequency. The output is the first derivative of the absorption spectrum. In this chapter, this method is referred to as *slow-scan EPR* or *CW EPR*.

Prior to the use of magnetic field modulation, EPR spectra were recorded as the voltage output of a diode detector, often called a *crystal detector*, as the magnetic field was swept. The signal was usually displayed on an oscilloscope. This is detection

at the resonance frequency, and is referred to as *direct detection*, as distinct from phase-sensitive detection at the field modulation frequency. The output is the absorption spectrum. Many such spectra are described in early papers [29, 52, 53]. This is also the detection method used in rapid-scan measurements – the signal is recorded directly with phase-sensitive detection at the resonance frequency using double-balanced mixer detection. The scans can be performed with magnetic field or microwave frequency sweeps such that the time on resonance is long or short relative to electron spin relaxation times. When the scan rate is slow relative to relaxation rates, and thus the time on resonance is long relative to the relaxation times, the absorption spectrum is detected. When the scan rate is fast and the time on resonance is short relative to relaxation times, oscillations may be observed on the trailing edge of the signal as shown in Figure 2.1. As the scan rate increases, the depth and number of oscillations increase and the signal broadens. Post-processing deconvolution can be used to remove both the broadening and the oscillations and obtain the undistorted absorption spectra [48]. Rapid scan is analogous to pulsed EPR in the sense that the microwaves are resonant with the spins for only a brief period during the scan. Consequently, much higher power can be used relative to a CW scan [10, 11, 54]. There is no magnetic field modulation broadening of the line. Examples in Section 2.12.5 show particularly large improvements in S/N for rapid scan relative to CW for species with long electron spin relaxation times.

In CW spectroscopy, if the time to scan through the signal is short relative to relaxation times, passage effects distort the lineshape [29]. This can make it difficult to record spectra of samples with long electron spin relaxation times such as the E′ defect in irradiated quartz [55], or for many samples at low temperatures. For example, at about 5 K the spin-lattice relaxation time of vanadyl porphyrin is so long that reversing the direction of the magnetic field scan inverts the EPR spectrum, which then looks similar to an absorption (or emission) spectrum even though it is a field-modulated first-derivative spectrum (e.g., see Figure 6 in [56]). Rapid-scan spectroscopy takes advantage of the passage effects, which can be removed by deconvolution, to obtain the undistorted absorption lineshape with enhanced signal intensity.

If standard CW EPR is performed with small enough modulation amplitude to faithfully define the derivative of the absorption signal, the amplitude of the phase-sensitive detected signal is about 1/10 or less of the maximum possible signal. One can use modulation amplitudes less than or equal to the linewidth and recover the undistorted signal post-acquisition [57–62], but there are limitations to the corrections that can be made. In addition, these corrections cannot compensate for passage effects.

In a rapid-scan experiment, the microwave power is applied to the spin system for a short time during the scan of the magnetic field through resonance. The faster the scan, the shorter the time during which B_1 excites the spins; therefore, the balance between excitation and relaxation favors relaxation, and higher B_1 can be applied. The dependence of signal amplitude on scan rate for LiPc (lithium phthalocyanine) is shown in Figure 2.2 [54]. If B_1 is constant, signal amplitude decreases with increasing scan rate because the signal does not have time to respond to B_1 during

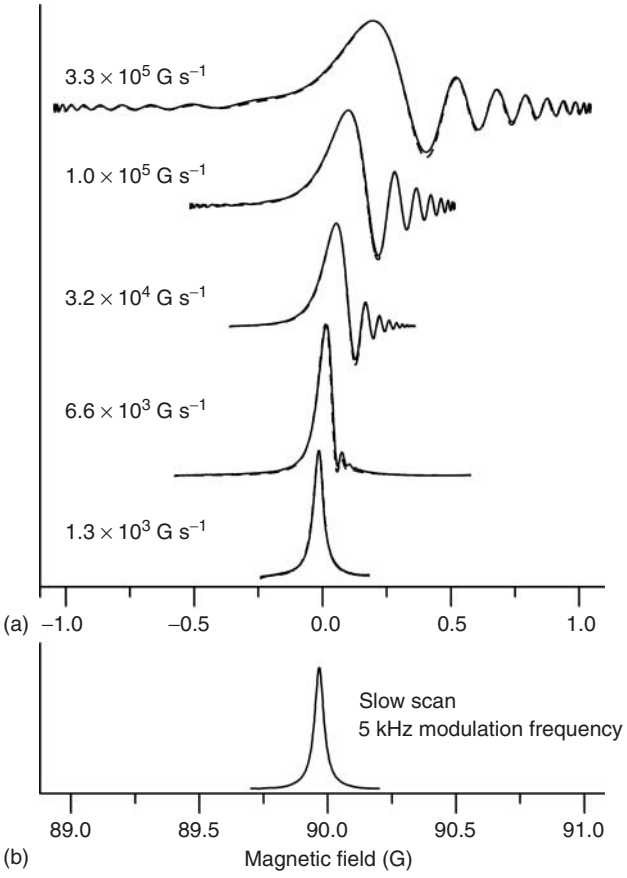

Figure 2.1 EPR spectra of LiPc at about 252 MHz. (a) Sinusoidal rapid-scan spectra obtained at the scan rates shown. The *x*-axis is the offset from resonance (in gauss) and the spectral widths of the traces are the scan widths. The number of scans averaged for each scan rate was selected to give a total signal acquisition time of 84 s. The *y*-axis scales are arbitrary. The values of B_1, selected to be a factor of 2 below the values that gave the maximum signal intensity, were: 4.6×10^{-2} G at 3.3×10^5 G s^{-1}, 2.6×10^{-2} G at 1.0×10^5 G s^{-1}, 1.8×10^{-2} G at 3.2×10^4 G s^{-1}, 1.15×10^{-2} at 6.6×10^3 G s^{-1}, and 4.6×10^{-3} G at 1.3×10^3 G s^{-1}. Simulated spectra (dashed lines) calculated using numerical integration of the Bloch equations are overlaid on the experimental data. (b) First integral of slow-scan CW spectrum obtained with 5 kHz modulation frequency, modulation amplitude of 10 mG, $B_1 = 4.6 \times 10^{-3}$ G, 84 s scan, 252.07 MHz. (Source: Stoner *et al*., 2004 [54]. Reproduced with permission of Elsevier Limited.)

the time on resonance. However, the maximum signal amplitude can be increased by increasing B_1 as the scan rate is increased. The transition from the regime where intensity is independent of scan rate to the regime where intensity is scan-rate dependent occurs when the scan rate satisfies the criterion shown in Eq. (2.1). Specific examples are shown in Section 2.12.

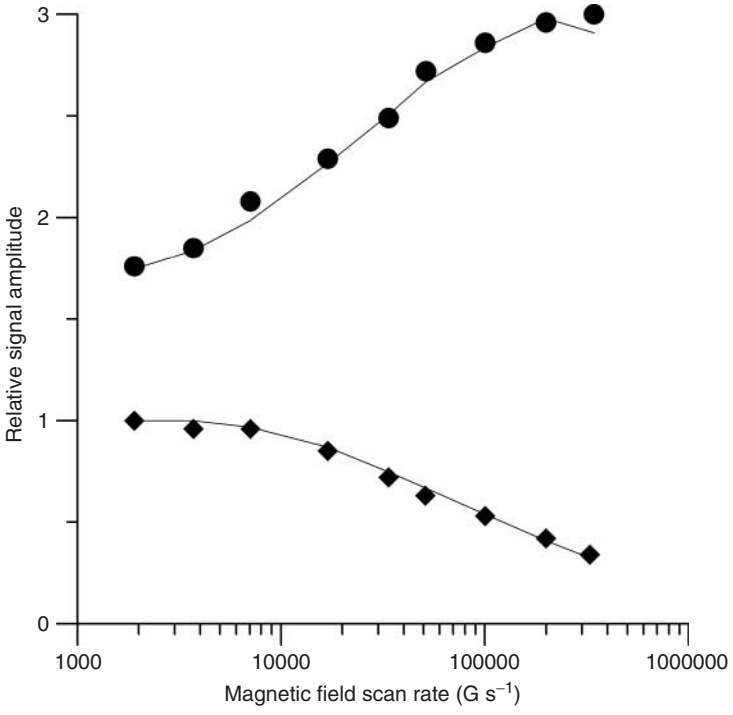

Figure 2.2 Relative intensities for the LiPc signal at the center of the sinusoidal scan as a function of scan rate at constant B_1 of 6.5×10^{-3} G (◆) and at the B_1 that gave the maximum signal amplitude (•). The number of scans was held constant. The relative signal amplitudes were scaled to 1.0 for the signal at constant B_1 of 6.5×10^{-3} G collected at the scan rate of 1.3×10^3 G s^{-1} (scan width of 0.42 G and scan frequency of 1 kHz). The solid lines connect points that were calculated by numerical integration of the Bloch equations (using the parameters for LiPc and the experimental scan widths and frequencies). (Source: Stoner *et al.*, 2004 [54]. Reproduced with permission of Elsevier Limited.)

A power saturation curve is a plot of signal amplitude as a function of microwave B_1. (Recall that B_1 is proportional to the square root of incident power.) To have integrated signal intensity proportional to the number of spins in the sample as is required for spin quantitation, both rapid-scan and CW require operation in the regime where signal amplitude increases linearly with B_1. For CW spectra, the power saturation curve is independent of scan rate. Because of the scan-rate dependence of signal amplitude shown in Figure 2.2, rapid-scan power saturation curves depend on scan rate as shown in Figure 2.3 for a nitroxide radical [10]. As the scan rate is increased, higher powers can be used without saturating the signal, and the maximum signal amplitude increases. The dashed lines in the figure are calculated power saturation curves based on simulations using time-dependent Bloch equations.

If the spectrum can be fully excited by the microwave pulse, pulsed EPR detects the full signal. Standard X-band pulsed EPR spectrometers using amplifiers that

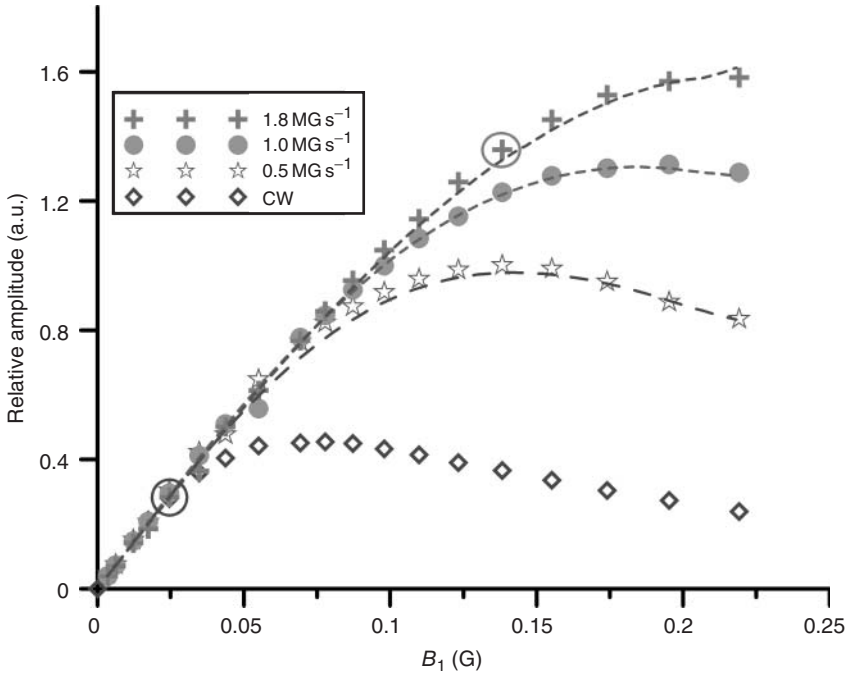

Figure 2.3 Amplitude of CW and rapid-scan spectra of the low-field nitrogen hyperfine line of 0.1 mM ^{15}N-mHCTPO solution as a function of microwave B_1. The scan widths were ~10 G and rapid-scan frequencies were 15.9, 31.5, or 57.4 kHz. Rapid-scan signals were 1024 averages, collected in less than 1 s. CW spectra were collected with a single scan acquired in ~82 s. The *y*-axis scale is the same for all of the rapid scans. The amplitude of the CW spectra is scaled to match that obtained for the rapid scans at low B_1. The dashed lines represent the calculated power saturation curves, which were simulated by numerical integration of the Bloch equations. The points selected for the acquisition conditions for rapid scan and CW spectra are circled. (Source: Mitchell *et al.*, 2012 [10]. Reproduced with permission of Elsevier Limited.)

can deliver tens to hundreds of watts microwave power to the resonator can generate 20 ns 90° pulses, which excite about 50 MHz of spectral width, provided that resonator Q is sufficiently low so that the bandwidth of the excitation is less than the resonator bandwidth. Some spectrometers can achieve shorter pulses with correspondingly larger spectral coverage. However, the relatively few spectra that are narrow enough to be fully excited with pulsed EPR can be studied with rapid-scan EPR with much lower power, and hence with instrumentation that is less expensive. Rapid scan can also be applied to spectra that are too wide to be fully excited by a 20 ns pulse. Pulsed EPR also is limited to signals with T_2* substantially longer than the dead time of the resonator, which is not a limitation for rapid scan.

In summary, the advantages of rapid scan relative to CW EPR arise from the detection of the full signal amplitude on every scan through the signal, the ability to use higher microwave powers, and the availability of deconvolution algorithms that take account of the known impact of passage effects on the signal.

2.1.3 Scan Types

The emphasis in this chapter is on magnetic field scans. The rate at which the field of an iron-core magnet can be scanned is relatively slow; therefore, scan coils are used to generate the rapidly changing fields. Scans have been primarily triangular or sinusoidal, but many other shapes have potential applications. In a triangular scan, the rate of scan is constant across the spectrum and is given by

$$a_t = 2f_s B_m (\mathrm{G\,s^{-1}}) \tag{2.3}$$

where a_t is the triangular scan rate, f_s is the scan frequency, and B_m is the scan width in gauss.

For a sinusoidal scan, the scan rate varies across the spectrum. The maximum rate at the center of the scan, a_s, is given by

$$a_s = \pi f_s B_m (\mathrm{G\,s^{-1}}) \tag{2.4}$$

As discussed in Section 2.5.2, resonating the coils with the driver circuit reduces the voltage requirements for scan generation, so it is easier to generate faster and wider sinusoidal scans than triangular scans.

Alternatively, the microwave frequency can be swept at constant magnetic field. The primary limitation on frequency scans is that the reflected microwave power and phase follows the resonator Q curve. The cavity reflection coefficient increases significantly at the extremes of the frequency sweep. The result is a frequency-dependent baseline. Since resonator $Q = \nu/\Delta\nu$, for the same resonator Q, the frequency bandwidth $\Delta\nu$ increases proportional to ν. Consequently, frequency sweep is more feasible at the high microwave frequencies used in high-field EPR. Hyde and coworkers [40] exploited the 1 GHz bandwidth of a W-band (95 GHz) resonator to perform rapid frequency sweep EPR. Frequency sweep rates with the yttrium iron garnet (YIG) oscillator were up to 1.8×10^5 GHz s^{-1}. Absorption and dispersion signals were obtained for the nitroxide CTPO (3-carbamoyl-2,2,5,5-tetramethyl-3-pyrrolinyl-1-oxy) and for mixtures of ^{14}N and ^{15}N-CTPO using triangular and trapezoidal waveforms (Figure 2.4).

The microwave frequency sweep can be very fast, as in a ''chirp'' of frequencies. Tseitlin *et al.* [63] demonstrated this capability with frequencies generated by an arbitrary waveform generator (AWG).

2.1.4 Digital Rapid Scan

Recent advances in digital electronics make it possible to develop a fully digital EPR spectrometer. A major advantage of a digital spectrometer is its flexibility to be configured, with little cost or effort, to do rapid-scan and pulse experiments at multiple frequencies with a single spectrometer, rather than requiring multiple stand-alone systems. It is possible to do a variety of experiments more efficiently,

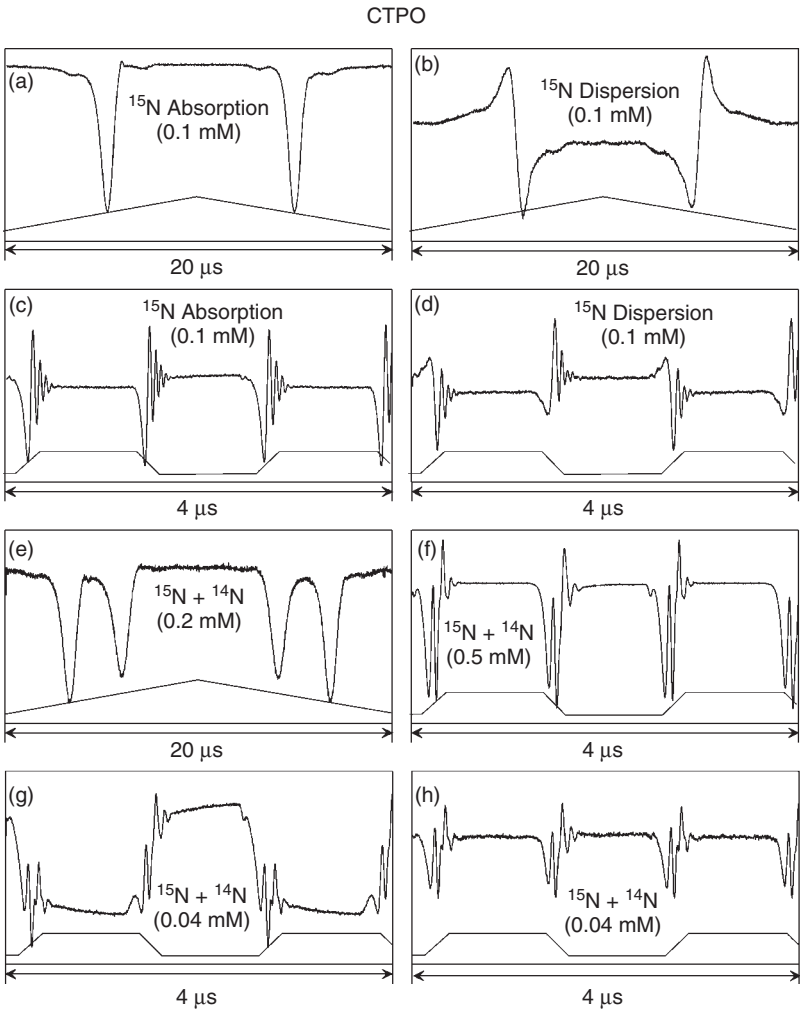

Figure 2.4 Representative swept-frequency responses for the CTPO sample. Parts (a) and (b) used 50 kHz triangular waveforms of 44.7 MHz deviation centered on the low-field line. Part (e) used 50 kHz triangular waveforms of 45.3 MHz deviation centered between the two low-field lines of ^{14}N and ^{15}N CTPO. Parts (c), (d), (f), (g), and (h) used the trapezoidal waveform of 36.7 MHz deviation centered on the low-field or between the two low-field lines of the ^{14}N and ^{15}N CTPO. Sweep rates are 0.147 MHz ns^{-1} (equivalent to 52.5 MG s^{-1}). Parts (c) and (h) are double-baseline corrected. (Source: Hyde *et al*., 2010 [40]. Reproduced with permission of Elsevier Limited.)

more accurately, with better S/N and at lower total cost. As a step in that direction, a comparison has been made of rapid-scan EPR spectra at 250 MHz with a traditional bridge and with a fully digital system. The 250 MHz excitation energy and the triangular rapid scan were generated with a Tektronix AWG.

The signal was amplified and digitally detected immediately after the resonator, without the use of a mixer. This approach eliminates the many complicated components of the "bridge" that are used in conventional EPR spectrometers. Tests were performed on samples with narrow lines including a trityl radical with well-resolved ^{13}C hyperfine splittings (Figure 2.5a), the nitroxide radical mHCTPO (4-protio-3-carbamoyl-2,2,5,5-tetraperdeuteromethyl-3-pyrrolinyl-1-oxy), which is used for oximetry (Figure 2.5b), and semiquinones with well-resolved proton hyperfine splittings.

2.1.5
Absolute Signal Quantitation

Quantitative EPR has long been recognized as difficult and subject to many confounding factors. Spin quantitation by EPR is typically done by comparison of the signal intensity of an unknown to that of a standard sample under comparable conditions. The goal of this study was to compare absolute experimental and theoretical signals and noise intensity for rapid scan at 250 MHz. The spectrometer, the resonator, and the sample were characterized in detail, which then permitted the measurement of any one of several free parameters, such as filling factor or B_1 for a particular incident power, which might otherwise be difficult to determine. These measurements are key to understanding the performance of the spectrometer and provide guidance in selecting the portions that are the most important targets for

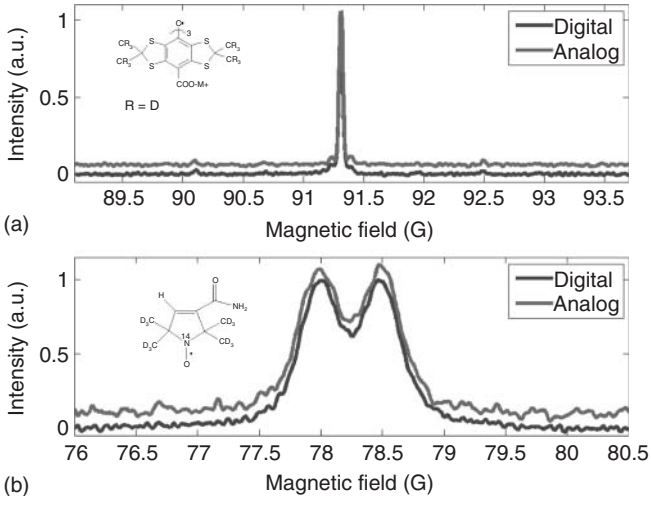

Figure 2.5 Analog and digital triangular rapid-scan EPR spectra at 256 MHz with a field scan width of 4.8 G and scan frequency of 4 kHz. (a) 0.2 mM aqueous trityl-CD_3 and (b) low-field nitrogen hyperfine line of 0.25 mM aqueous ^{15}N-mHCTPO. The doublet splitting is due to the single proton at position 4 of the ring. In each panel the upper scan is analog and the lower one is digital. (Source: Tseitlin *et al.*, 2011 [63]. Reproduced with permission of Elsevier Limited.)

improvement [64]. This study extended the approach of prior studies by the Denver laboratory of spin echo amplitudes to rapid-scan EPR.

The calculation of signal and noise yielded an $S/N = 1.92$ for about 0.64 cm^3 of 0.43 mM aqueous tempone-d_{16} in a 10 mm o.d. sample tube at 258.5 MHz. The experimentally measured value was $S/N = 2.07$, in excellent agreement. It should be noted that although the S/N agreement is unexpectedly good, the experimental measurements of both signal and noise are about 4% lower than the theoretical values. This is attributed to errors in characterizing the bridge gain and noise figure and the fact that these values are interdependent. The experiment and calculation demonstrate the ability to fully characterize a spectrometer, resonator, and sample system [64].

2.1.6
Signal-to-Noise Advantage of Rapid Scan Relative to CW

As discussed in Section 2.1.2, the rapid-scan method detects the absorption signal and CW spectroscopy detects the first derivative of the absorption. EPR spectroscopists are accustomed to viewing first-derivative displays of data. However, uncertainty analysis has shown that when spectral simulation is used to analyze data with the same S/N, (i) the linewidths can be obtained with the same uncertainties from absorption and first-derivative spectra, and (ii) the spin concentrations can be calculated more accurately from the absorption spectrum than from the first derivative [65]. Taking a derivative enhances high-frequency noise, and integration of the first derivative to obtain the absorption signal emphasizes low-frequency noise. Thus, interconversion between absorption and first-derivative signal displays changes the noise spectrum of the data. Therefore, in comparing rapid-scan and CW spectra it is appropriate to compare the S/N in the original data acquisition forms, which is the first derivative for CW and absorption for rapid scan.

Comparison of S/N for rapid-scan and CW spectra includes three factors: (i) differences in signal amplitudes detected with phase-sensitive detection at the modulation amplitude and direct detection, (ii) the signal-amplitude advantage from rapid scanning in the regime where increasing scan rate and increasing B_1 increases signal amplitude, and (iii) the noise in CW and rapid-scan spectra. These three factors are described in detail in the following paragraphs.

1) In CW with phase-sensitive detection at the magnetic field modulation frequency, when the magnetic field is set to the position with maximum signal, the time-dependent spin response, $R(t)$, is given by

$$R(t) = \frac{1}{2} r_m \cos(2\pi f_m t) \tag{2.5}$$

where r_m is the peak-to-peak amplitude of the response and f_m is the modulation frequency. Phase-sensitive detection, either in hardware or in software, consists of two steps [66]. Step 1 of phase-sensitive detection is multiplication of $R(t)$ by the reference signal $\cos(2\pi f_m t)$, which produces sum and difference

frequencies, each of which has half of the original amplitude. The sum is at twice the modulation frequency and the difference is at the baseband. Step 2 is low-pass filtering, which eliminates signal at the second harmonic and suppresses high-frequency noise. The net result is a down-conversion of the spectrometer response to baseband. The resulting signal has an amplitude of $r_m/4$, which corresponds to a peak-to-peak amplitude of $r_m/2$ of the first derivative (Figure 2.6a).

In a rapid-scan experiment, the field is swept through resonance twice during the full scan cycle. The full amplitude of the absorption signal (A_a) is detected, which is larger than the maximum amplitude detected with field modulation by a factor of $A_a/r_m = D$ (Figure 2.6a). The ratio of the amplitudes of the rapid scan and CW spectra is, therefore, $(D\, r_m)/(r_m/2) = 2D$. For conservative choices of modulation amplitudes, D may be as large as 5 or 10. For a strongly overmodulated signal, D is still about 2. Thus, $2D$ is a substantial advantage in signal amplitude, which is due to direct detection, independent of whether the scan time is short or long relative to relaxation times.

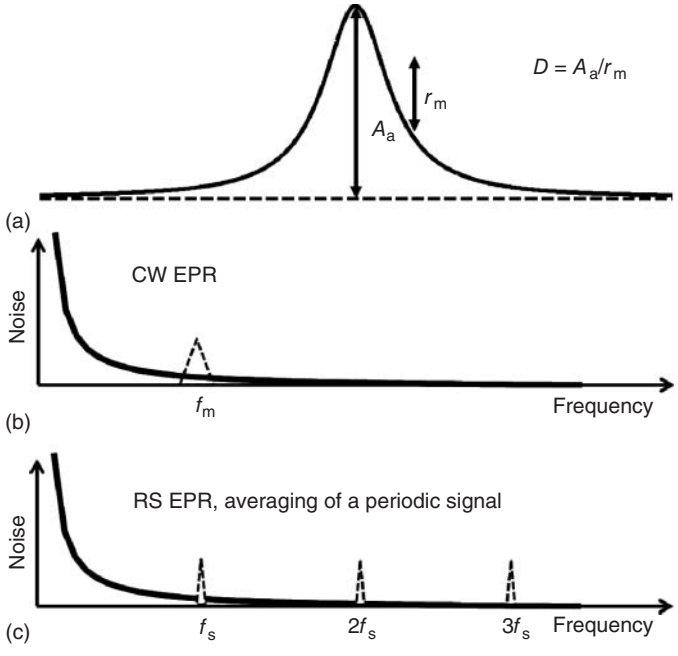

Figure 2.6 (a) Comparison of signal amplitudes detected by rapid scan (A_a) and CW spectroscopy (r_m). (b) Comparison of noise reduction in CW and rapid-scan averaging. A hypothetical spectrometer noise profile relative to the carrier in the frequency domain is shown as a solid line. In CW the field modulation and phase-sensitive detection at the modulation frequency, f_m, shift the noise profile in the data away from that at the carrier by the offset f_m. (c) The averaging of a periodic signal in rapid scan shifts the noise profile to a comb of frequencies at multiples of the scan frequency, f_s. The noise bandwidths of the combs (Eq. (2.7)) are narrower than the noise bandwidths for CW EPR.

2) As discussed in Section 2.1.2, higher microwave powers can be used in rapid scans without saturating the signal (Figure 2.3), which produces higher signal amplitudes. This has been demonstrated for trityl radicals [54], LiPc [54], the E′ signal in irradiated fused quartz [45], nitroxide radicals [10], and paramagnetic centers in materials [11]. The extent of signal enhancement, $F = A_a(\textit{rapid scan})/A_a(\textit{direct-detected slow scan})$, depends on relaxation times and scan rates. For the nitroxide example shown in Figure 2.3, F is about 4. The combined signal enhancement that can be achieved by rapid scanning, by a factor of F, and direct detection, by a factor of $2D$, is then $2DF$.
3) The noise in the two types of experiments also needs to be considered. The use of field modulation and phase-sensitive detection at the modulation frequency reduces signal, but it also reduces noise. Noise in experimental data is not white. In addition to thermal noise (which is always present), there may be substantial contributions from source noise, which is highest near the carrier frequency. Use of field modulation offsets the EPR signal in the frequency domain by f_m (Figure 2.6). If the modulation frequency is high enough, the detected signal is moved into the region where the noise spectrum is flat and noise is approximately white.

In rapid scans the source noise is reduced by averaging of a periodic signal. This time domain averaging is equivalent to applying a comb filter $H(f)$ in the frequency domain (Figure 2.6c). The absolute value of the filter function is

$$|H(f)| = \frac{\sin(N_{aver})\frac{\pi f}{f_s}}{\sin\left(\frac{\pi f}{f_s}\right)} \tag{2.6}$$

where f_s is the scan frequency. Noise components that are not coherent with the periodic signal are efficiently attenuated. The width of each comb is equal to the inverse of the total averaging time, *Time*, in Eq. (2.7).

$$\Delta f = \frac{f_s}{N_{aver}} = \frac{1}{\textit{Time}}, \tag{2.7}$$

where N_{aver} is the number of scans averaged. This is a much narrower filter bandwidth than that used in CW experiments. Coherent averaging of the periodic rapid-scan signal offsets the signal in the frequency domain to the region of the noise spectrum where the noise spectrum is approximately frequency independent (Figure 2.6). The quantitative impact of the narrower comb filter has not been estimated, so it is not included in the overall comparison of CW and rapid-scan spectra. This principle was demonstrated by Klein and Barton in 1963 [67] for NMR spectra that included ''wiggles'' and for CW EPR spectra.

If CW and rapid-scan experiments are performed in the regime where both f_m and f_s are high enough to shift the spectrum into the regime where the noise is approximately independent of frequency, the white noise approximation can be used to compare two experiments performed on the same spectrometer. Before detection, both CW and rapid scan have noise with the same standard deviation, σ. In the phase-sensitive detection of the CW spectrum, multiplication by $\cos(2\pi f_m t)$